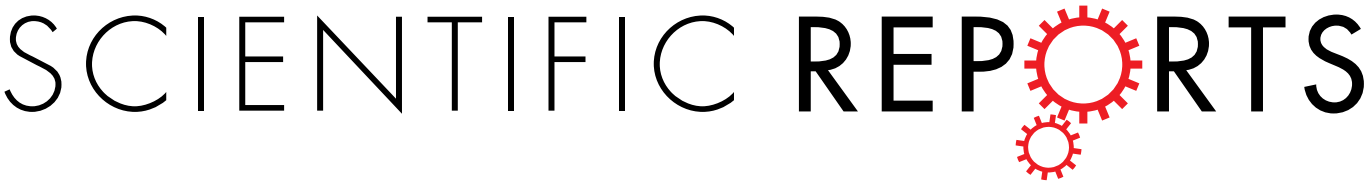

OPEN

Visualization of ligand-induced dopamine D_{2S} and D_{2L} receptor internalization by TIRF microscopy

Received: 16 March 2017
Accepted: 23 August 2017
Published online: 07 September 2017

Alina Tabor[1], Dorothee Möller[1], Harald Hübner[1], Johannes Kornhuber[2] & Peter Gmeiner[1]

G protein-coupled receptors (GPCRs), including the dopamine receptors, represent a group of important pharmacological targets. Upon agonist binding, GPCRs frequently undergo internalization, a process that is known to attenuate functional responses upon prolonged exposure to agonists. In this study, internalization was visualized by means of total internal reflection fluorescence (TIRF) microscopy at a level of discrete single events near the plasma membrane with high spatial resolution. A novel method has been developed to determine the relative extent of internalized fluorescent receptor-ligand complexes by comparative fluorescence quantification in living CHO cells. The procedure entails treatment with the reducing agent sodium borohydride, which converts cyanine-based fluorescent ligands on the membrane surface to a long-lived reduced form. Because the highly polar reducing agent is not able to pass the cell membrane, the fluorescent receptor-ligand complexes located in internalized compartments remain fluorescent under TIRF illumination. We applied the method to investigate differences of the short (D_{2S}) and the long (D_{2L}) isoforms of dopamine D_2 receptors in their ability to undergo agonist-induced internalization.

G protein-coupled receptors (GPCRs) represent a large family of integral membrane proteins and their primary function is to transduce extracellular stimuli (e.g ligand binding) into intracellular signals[1]. These receptors play fundamental roles in many physiological and pharmacological processes and therefore serve as important drug targets which are addressed by more than 30% of the current drugs on the market[2]. Dopamine D_2 receptors, which belong to the family of class A GPCRs, mediate various physiological functions and are known as valuable targets for the treatment of neuropsychiatric disorders including schizophrenia, Parkinson's disease and drug addiction[3–8].

D_2 receptors exist in two splice variants, the short (D_{2S}) and the long (D_{2L}) isoform, which have been suggested to be localized pre- and postsynaptically, respectively[9]. Although different spatial distributions and functions have been suggested, the individual contributions of the two isoforms to (patho)-physiological processes remain unclear.

Following agonist stimulation, GPCRs undergo conformational changes that allow binding and activation of heterotrimeric G proteins. Subsequently, the Gα and Gβγ subunits modulate a variety of signaling events within the cell. Importantly, GPCRs undergo a highly dynamic regulation upon activation. Multiple mechanisms provide control over the specificity and extent of the cellular response. For instance, agonist stimulation of receptors at the cell surface can induce receptor desensitization and, consequently, receptor internalization through different endocytotic pathways[10,11]. Agonist activation of most GPCRs leads to phosphorylation of the receptors by G protein-coupled receptor kinases (GRKs). GKRs and β-arrestins, together orchestrate receptor uncoupling from the G protein and thereby terminate G protein signaling[12,13]. In many cases, β-arrestin recruitment leads to receptor internalization, which generally proceeds by clathrin-coated pits or other mechanisms of endocytosis[14–16], in which the receptors are translocated away from the plasma membrane to lager intracellular vesicular or endosomal structures. Once internalized, GPCRs are either dephosphorylated and recycled back to the plasma membrane, or targeted to lysosomes for proteolysis, which results, in part, in receptor downregulation[17]. Interestingly, recent reports have demonstrated that canonical GPCR signaling may also occur from internalized GPCRs in endosomes[18–21].

[1]Department of Chemistry and Pharmacy, Emil Fischer Center, Friedrich-Alexander University Erlangen-Nürnberg, Schuhstraße 19, 91052, Erlangen, Germany. [2]Department of Psychiatry and Psychotherapy, Friedrich-Alexander University Erlangen-Nürnberg, Schwabachanlage 6, 91054, Erlangen, Germany. Correspondence and requests for materials should be addressed to P.G. (email: peter.gmeiner@fau.de)

Various experimental approaches have been utilized to measure GPCR ligand binding and internalization. Among them are, in particular, radioligand binding studies, enzyme-linked immunoabsorbent assays (ELISA) and fluorescent immunocytochemistry experiments[22–24]. However, as a principal limitation these protocols generally require fixation and/or permeabilization of cells. Other approaches for directly measuring receptor internalization include microplate-based functional cell assays build upon enzyme fragment complementation, bioluminescence- and fluorescence-resonance energy transfer technologies (BRET and FRET)[25–27]. Moreover, alternative strategies based on fluorescence microscopy using fluorescent protein tags have been followed to monitor internalization in living cells[28,29].

Fluorescence microscopy facilitates a novel way to study ligand binding and the subsequent internalization process of GPCRs in living cells, using fluorescence-based probes such as fluorescent ligands[30]. In particular, total internal reflection fluorescence (TIRF) microscopy has proved useful to study internalization because of its ability to selectively detect both fluorescent molecules situated within or in close proximity (~100 nm) to the plasma membrane with high spatial and temporal resolution[18,31,32].

Taking advantage of our recently developed high affinity fluorescent dopamine receptor agonists and antagonists[33], we visualize internalization by means of TIRF microscopy at a level of discrete single events near the plasma membrane. Employing the reducing agent sodium borohydride ($NaBH_4$), which converts cyanine-based fluorescent dyes on the membrane surface to a long-lived reduced form, we herein present a novel method to determine the relative proportion of internalized fluorescent receptor-ligand complexes by comparative fluorescence quantification under living cell conditions. Using this method, we are able to investigate differences of the two dopamine D_2 receptor isoforms, D_{2S} and D_{2L}, in their ability to undergo agonist-induced internalization.

Results

Direct visualization of agonist-induced cluster formation of D_{2S} and D_{2L} receptors. Very recently, we reported on the pharmacological characterization of Cy3B-conjugated fluorescent antagonists (**1a**,**b**) and agonists (**2a**,**b**) targeting dopamine D_2/D_3 receptor subtypes (Fig. 1a)[33]. These four fluorescent ligands were shown to possess binding affinities in the low nanomolar range (Supplementary Table S1) and their suitability for live-cell fluorescence microscopy with excellent signal to noise ratios and high temporal and spatial resolution could be demonstrated[33].

Initial TIRF microscopy experiments in this study showed that receptor-ligand complexes of the fluorescent antagonists **1a** and **1b** bound to dopamine D_{2S} or D_{2L} receptors stably expressed in CHO cells (10 nM, for 1 h at 37 °C) were visible under TIRF illumination as individual, freely diffusing, diffraction limited spots. These spots were homogeneously distributed over the membrane of the living CHO cells (representative for **1b**, see Fig. 1b,c, Supplementary Movie S1). Interestingly, cells incubated with the fluorescent agonists **2a**,**b** showed an inhomogeneous labeling distribution (representative for **2b**, see Fig. 1d,e, Supplementary Movie S2). In addition to the labeled receptors on the membrane surface, fluorescent puncta were observed, which were predominantly clustered. In contrast to the diffraction-limited spots of single ligand-receptor complexes (Fig. 1f), these fluorescent puncta could not be treated as diffraction-limited spots and showed confined diffusive behavior and increased intensities (Fig. 1g). Moreover, the TIRF experiments revealed that the short and long isoforms of the D_2 receptors (D_{2S} and D_{2L}) differ in their ability to form the clustered fluorescent puncta (Fig. 1d,e). These findings could not be attributed to differences in receptor expression as the experiments were performed with monoclonal CHO cell lines with nearly identical expression levels of the D_{2S} or D_{2L} receptors, respectively (B_{max} of 970 ± 60 fmol mg^{-1} protein for D_{2S} and 1060 ± 60 fmol mg^{-1} protein for D_{2L})[33].

To further investigate this initial observation, CHO cells stably expressing D_{2S} receptors were pretreated with an excess of the unlabeled antagonist spiperone (10 µM, 2 h at 37 °C), followed by the incubation with the fluorescent agonist **2b** (10 nM, 1 h at 37 °C). When these cells were imaged under TIRF illumination, neither clustered fluorescent puncta nor labeling of the receptors at the cell surface were observed, indicating that unspecific binding and uptake of ligand **2b** were negligible (Supplementary Fig. S1). Thus, we hypothesized that the fluorescent agonists **2a**,**b** were internalized into the living CHO cells in a dopamine D_2 receptor specific manner.

ELISA-detected internalization and β-arrestin recruitment. In order to associate our initial findings, the significant agonist-induced relocalization of D_2 receptors, with the GPCR internalization process, we used a classical ELISA (enzyme-linked immunosorbent assay) approach[34]. Therefore, the decrease of cell surface expression of FLAG-tagged D_{2S} or D_{2L} receptors was quantified in response to treatment with fluorescent agonists (**2a**,**b**) in transiently transfected HEK cells (Fig. 2a,b). At a concentration of 1 µM, both fluorescent agonists induced internalization of dopamine D_{2S} and D_{2L} receptors, respectively, highly similar to a reference agonist quinpirole (10 µM) (remaining surface expression for D_{2S}: 68 ± 5% quinpirole, 67 ± 3% **2a**, 67 ± 4% **2b**; and D_{2L}: 71 ± 5% quinpirole, 67 ± 4% **2a**, 64 ± 6% **2b** (mean ± s.e.m)). Comparable results were also obtained when concentrations identical with those used within TIRF microscopy experiments (10-fold of K_i concentration) were applied in the internalization assay (remaining surface expression for D_{2S}: 69 ± 7% quinpirole, 68 ± 3% **2a**, 62 ± 5% **2b**; and D_{2L}: 69 ± 8% quinpirole, 76 ± 8% **2a**, 66 ± 7% **2b** (mean ± s.e.m), Fig. 2a,b).

Although different mechanisms ultimately leading to receptor internalization have been described, we were interested if our fluorescent agonists are able to engage the most prevalent and best characterized pathway for GPCR desensitization: the recruitment of β-arrestins to ligand-activated receptors[35–37]. Employing a commercially available test system based on enzyme-fragment complementation (DiscoverX PathHunter assay), we found that the agonists **2a** and **2b** stimulate substantial recruitment of β-arrestin-2 at D_{2S} and D_{2L} receptors(D_{2S}: $EC_{50} = 240 \pm 70$ nM, $E_{max} = 87 \pm 4$% and $EC_{50} = 230 \pm 60$ nM, $E_{max} = 75 \pm 7$%, for **2a** and **2b**, D_{2L}: $EC_{50} = 400 \pm 60$ nM, $E_{max} = 83 \pm 7$%, and $EC_{50} = 230 \pm 30$ nM, $E_{max} = 96 \pm 4$%, for **2a** and **2b** (mean ± s.e.m)), while the antagonists **1a** and **1b** were devoid of intrinsic activity (Fig. 2c,d and Supplementary Table S1). Compared to the reference agonist quinpirole (D_{2S}: $EC_{50} = 79 \pm 9$ nM, $E_{max} = 100 \pm 1$% and D_{2L}:

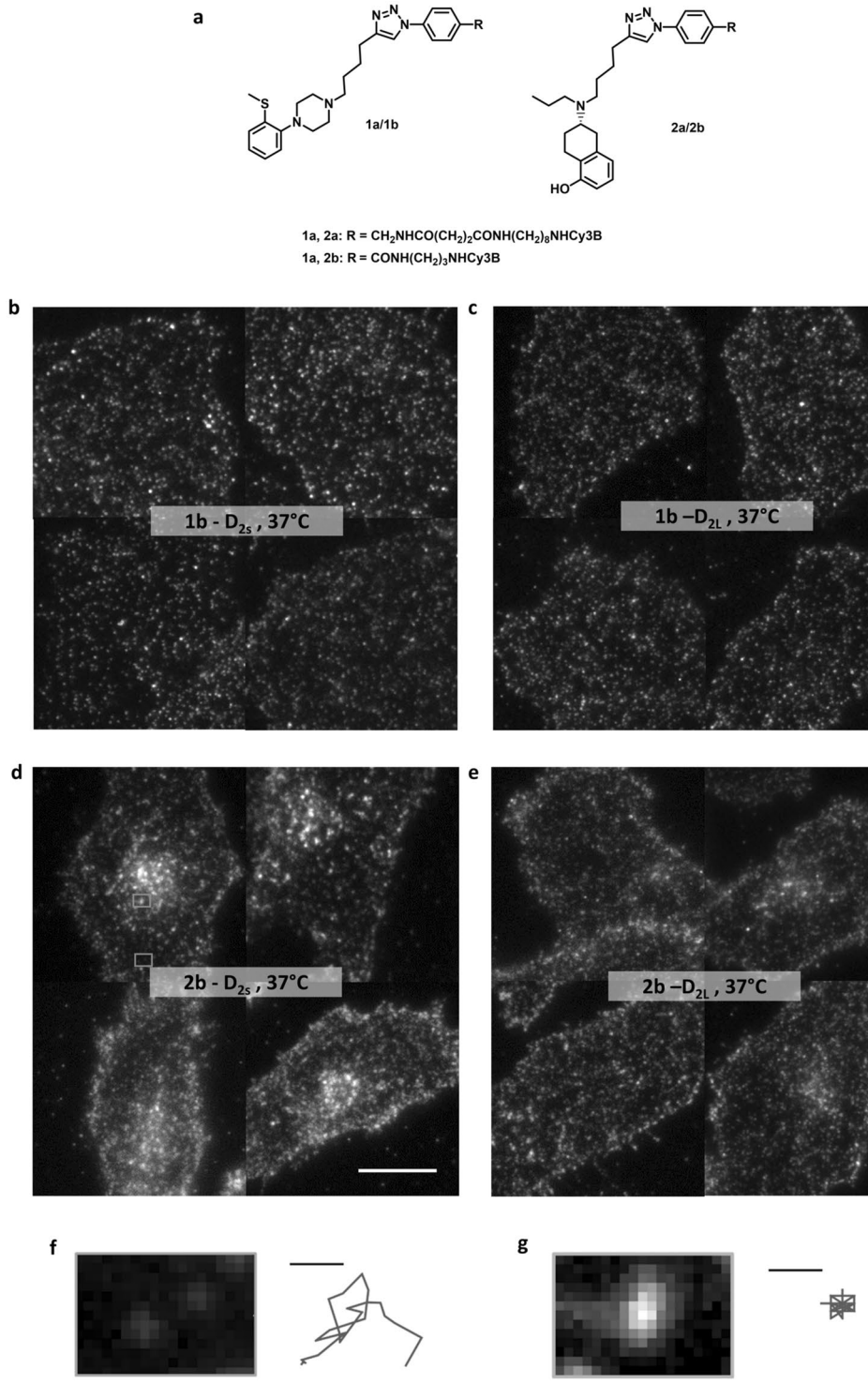

Figure 1. Visualization of agonist-induced dopamine D_{2S} and D_{2L} receptor fluorescent cluster formation in stably transfected CHO cells. (**a**) Chemical structure of the fluorescent antagonists (1a,b) and agonists (2a,b). (**b–e**) Representative TIRF images of CHO cells stably expressing D_{2S} or D_{2L} receptors exposed to the fluorescent antagonist 1b (10 nM) or agonist 2b (10 nM) for 1 h at 37 °C. Scale bar, 10 µm. (**f,g**) Intensity and position (left) and tracked path (right) of the selected fluorescent spots revealed different diffusive behavior (**f**, single ligand-receptor complexes in the cell membrane; **g**, cluster of ligand receptor complexes). Scale bar, 1 µm.

$EC_{50} = 110 \pm 10$ nM, $E_{max} = 100 \pm 1\%$ (mean ± s.e.m)) both, efficacies and potencies were found to be slightly reduced. Together, the results from ELISA-based internalization assays and β-arrestin-recruitment studies indicate that the fluorescent agonists **2a**,**b** are able to stimulate receptor desensitization and trafficking while the

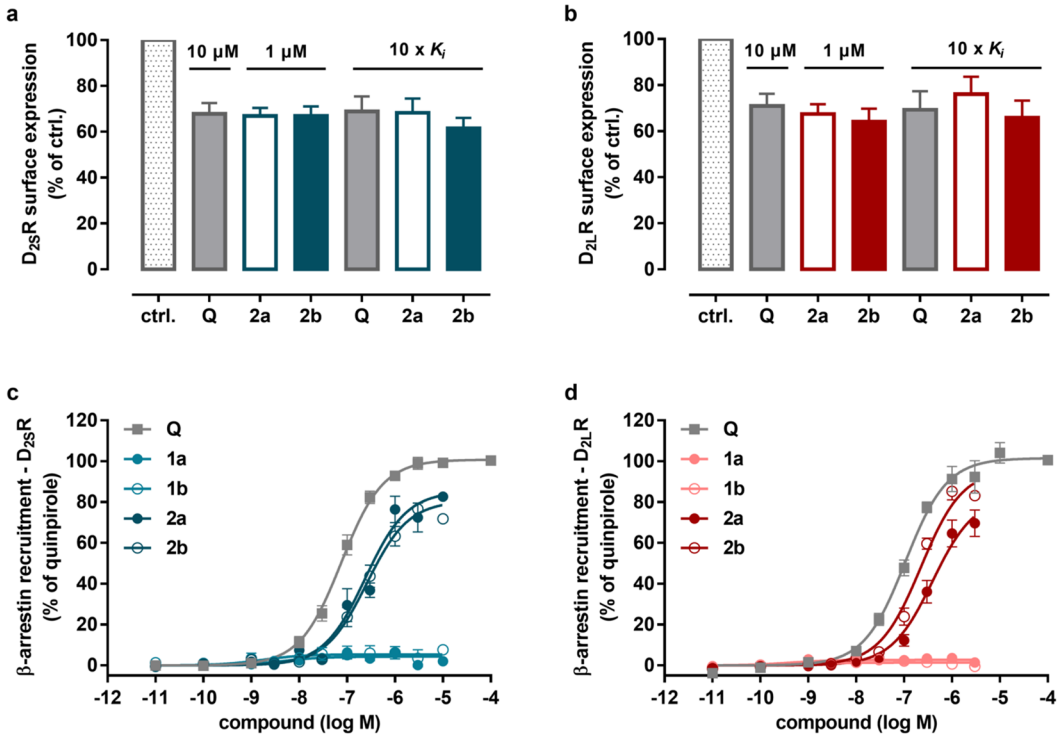

Figure 2. Agonist-induced internalization by cell surface ELISA and β-arrestin-2 recruitment at D_{2S} and D_{2L} receptors. N-terminally FLAG-tagged D_{2S} (**a**) and D_{2L} (**b**) receptors were transiently expressed in HEK cells and surface expression was examined after treatment with the reference agonist quinpirole (Q) or the fluorescent agonists (**2a**,**b**) for 1 h at 37 °C with the concentrations indicated. All ligands induced significant receptor internalization compared to vehicle (ctrl., one way-ANOVA followed by Dunnet's posthoc test, $p < 0.05$). Data represent mean ± s.e.m. of $n \geq 4$ independent experiments, each performed in quintuplicates. β-Arrestin-2 recruitment was determined employing the DiscoverX PathHunter assay. HEK cells stably expressing β-arrestin-2 tagged with the EA-fragment were transfected with ProLink-tagged D_{2S} (**c**) or D_{2L} (**d**) receptors, respectively. The fluorescent agonists **2a** and **2b** stimulate β-arrestin-2 recruitment dose-dependently and display almost full agonist activity. The fluorescent antagonists **1a** and **1b** do not induce β-arrestin-2 recruitment. Data represent mean ± s.e.m of $n \geq 3$ independent experiments, each performed in duplicate. Results were normalized to the maximum effect of the reference agonist quinpirole (100% for D_{2S} and D_{2L} receptors).

fluorescent antagonists **1a**,**b** do not induce these processes. Thus, we hypothesized that the occurrence of fluoresccent puncta observed by TIRF microscopy in presence of the agonists **2a**,**b** but not the antagonists **1a**,**b** may be related to these processes.

Control of clustered receptor-ligand complexes by temperature. Several studies have shown that endocytosis and trafficking mechanisms are blocked at reduced temperatures[38,39]. Indeed when we decreased the incubation temperature from 37 °C to ambient temperature (22–24 °C), the number of intracellular fluorescent puncta was significantly reduced after treatment of D_{2S} and D_{2L} with the fluorescent agonist **2b** (10 nM, Supplementary Fig. S2). The spot density corresponding to **2b**-D_{2L} complexes at the cell surface (0.65 ± 0.03 spots µm^{-2}, mean ± s.d. of 10 cells) was found to be highly comparable to that of antagonist **1b**-D_{2L} complexes (0.67 ± 0.03 spots µm^{-2}, mean ± s.d. of 10 cells, Fig. 1c).

Determination of the relative extent of internalized receptor-ligand complexes. To further explore the origin of the differences in the ability of D_{2S} and D_{2L} receptors to form clustered fluorescent puncta upon fluorescent agonist-binding, we developed a new method allowing to distinguish receptors on the cell surface from receptors internalized to intracellular compartments in living cells. The procedure entails treatment with the reducing agent sodium borohydride ($NaBH_4$), which converts the cyanine-based fluorescent dyes to a long-lived reduced form. Because the highly polar $NaBH_4$ is not able to pass the cell membrane, ligands bound to internalized receptors should be not affected by the treatment. Thus, the internalized Cy3B-conjugated ligands located in internalized compartments (endosomes) should remain fluorescent under TIRF illumination (Fig. 3a).

In order to prove that the fluorescence intensity of the Cy3B-conjugated ligands is negligible after reduction with $NaBH_4$, we performed *in vitro* control experiments. Thus, we added $NaBH_4$ (final concentration 30 mM) to an aqueous solution of the fluorescent antagonist **1a** (1 µM in dPBS) and measured an emission scan ($\lambda_{ex} = 530$ nm) with a spectrofluorimeter after 5 min. In agreement with previous reports on the reduction of cyanine dyes[40,41], the hydro-form of **1a** displayed non-fluorescent properties (Fig. 3b,c).

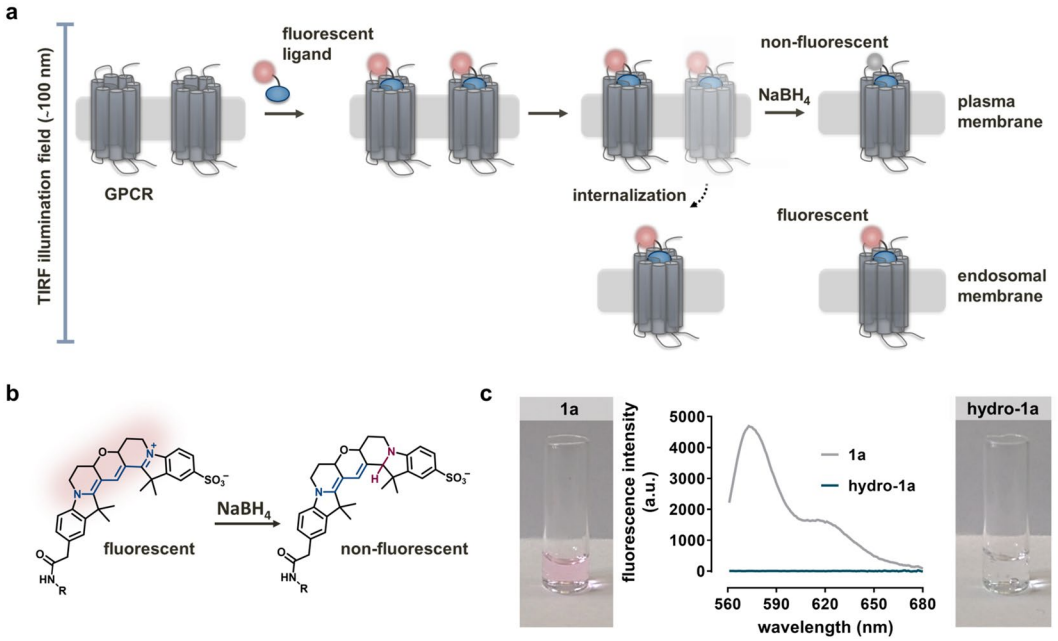

Figure 3. Reductive treatment approach. (**a**) Schematic illustration of the reductive treatment approach for the determination of the relative proportion of internalized receptor-ligand complexes. (**b**) Proposed structure of the non-fluorescent hydrocyanine after treatment of the fluorescent cyanine (Cy3B) with $NaBH_4$. (**c**) Spectroscopic validation of the reductive treatment of the Cy3B-conjugated fluorescent ligand **1a** with $NaBH_4$. Emission spectra ($\lambda_{ex} = 530$ nm) of the Cy3B-conjugated ligand **1a** in the presence and absence of $NaBH_4$ (30 mM) in dPBS. **Hydro-1a** shows negligible fluorescence emission.

To demonstrate the suitability of the reductive treatment procedure under living cell conditions, CHO cells stably expressing the D_{2S} receptor were incubated with the fluorescent ligands **1a** (antagonist) and **2b** (agonist) at a concentration of 10 nM for 1 h, followed by the treatment with 30 mM $NaBH_4$ for 5 min. Images of the cells were acquired before and after $NaBH_4$-treatment under TIRF illumination (Fig. 4a). As expected, for the fluorescent antagonist **1a** treatment with $NaBH_4$ reduced the initial fluorescence corresponding to receptor surface-bound fluorescent ligands to a nearly undetectable level. However, TIRF images of **2b**-labeled cells after $NaBH_4$ treatment revealed fluorescent puncta, indicating that the fluorescence results from reduction-resistant **2b**-receptor complexes localized in intracellular compartments (Fig. 4a).

The dynamics of these internalized compartments under TIRF illumination suggests that the cell treatment with $NaBH_4$ has minor effects on the cell viability (Supplementary Movie S3). Bright field images of the $NaBH_4$-treated cells also showed no significant changes in cell morphology or adhesive behavior.

To determine the relative extent of internalization, the reductive treatment approach was applied and evaluated by fluorescence quantification. Therefore, CHO cells stably expressing either D_{2S} or D_{2L} receptor were incubated for 1 h with the corresponding fluorescent ligands (**1a**,**b** or **2a**,**b**) at a concentration corresponding to the tenfold of the K_i value at 37 °C (Supplementary Table S1). Cells of each condition were imaged under TIRF illumination before and after $NaBH_4$ treatment.

The mean fluorescence intensity of a fluorescent ligand-labeled cell after $NaBH_4$ treatment was used to quantify fluorescence in the intracellular TIRF illumination field. The ratio of the intracellular fluorescence and the total fluorescence of the same cell before $NaBH_4$ treatment was used as a measure of receptor internalization. Importantly, TIRF microscopy only visualizes the peripheral cytoplasm (~100 nm from the basolateral membrane) and thus cannot be used to quantify the total amount of internalized receptors within an entire cell. However, the relative ratio of intracellular to total fluorescence can be applied to compare the internalization behavior of two different systems (e.g. receptor subtypes or ligands).

Figure 4b summarizes the results of the experiments described above. The extent of agonist-induced D_{2S}-mediated internalization was found to be significantly higher (**2a**: 35.3 ± 4.2% and **2b**: 32.9 ± 1.9% (mean ± s.e.m.)) than for the D_{2L} receptor isoform (**2a**: 16.3 ± 1.5% and **2b**: 19.8 ± 1.5% (mean ± s.e.m.)). The fluorescent antagonists **1a** and **1b** were not able to promote D_{2S} and D_{2L} receptor internalization (D_{2S}-**1a** 1.1 ± 0.9%, D_{2S}-**1b** 1.4 ± 1.3%, D_{2L}-**1a** 1.9 ± 0.4% and D_{2L}-**1b** 0.4 ± 1.5% (mean ± s.e.m)).

Discussion

There are still many open questions regarding the regulatory mechanisms involved in the downregulation of activated GPCRs including receptor internalization and signal termination[18–21]. Some of these questions can be addressed by fluorescence single-molecule imaging of GPCRs and their signal transducers with suitable fluorescent probes[18,42]. In particular, TIRF microscopy offers the possibility of studying membrane proteins with higher spatial and temporal resolution than conventional epifluorescence or confocal fluorescence microscopy.

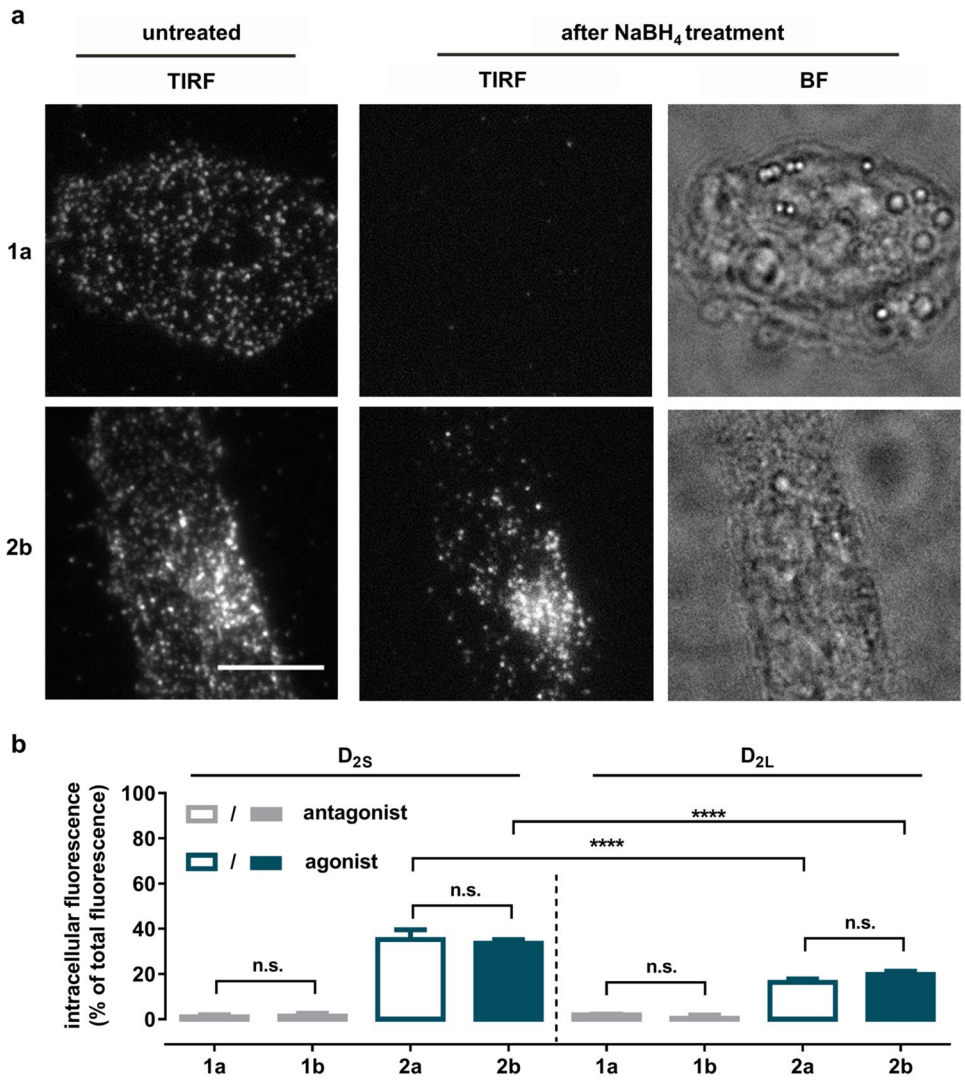

Figure 4. Ligand-induced internalization of D_{2L} and D_{2S} receptors. (**a**) Validation of the reductive treatment approach of **1a** and **2b** labeled D_{2S} receptors in living cells by TIRF microscopy. TIRF and brightfield (BF) images of CHO cells stably expressing the D_{2S} receptor incubated with the fluorescent ligand **1a** and **2b** for 1 h at 37 °C before and after treatment with $NaBH_4$. Scale bar, 10 µm. (**b**) Determination of the relative extent of internalized fluorescent receptor-ligand complexes. CHO cells stably expressing D_{2S} or D_{2L} receptors, respectively, were incubated for 1 h at 37 °C with the corresponding fluorescent ligands (concentration corresponding to the tenfold of the respective K_i value) and were imaged under TIRF illumination before and after $NaBH_4$ treatment (30 mM, 5 min). Data represent the fraction (%, mean ± s.e.m) of $NaBH_4$ inaccessible (internalized) mean fluorescence intensity of a fluorescently-labeled cell relative to the total cell's mean fluorescence intensity before the $NaBH_4$ treatment. At least three independent experiments were performed, with four or more cells imaged per condition. Statistical analysis was performed by an unpaired *t*-test, ****p-value < 0.0001, n.s. - not significant).

Moreover, events occurring within the plasma membrane like receptor-dimerization[33,43,44] or in close proximity to the membrane such as internalization can be studied in living cells under nearly physiological conditions[32,45].

Very recently, we have demonstrated that the fluorescent dopamine receptor antagonists **1a**,**b** and agonists **2a,b** can be used to directly visualize ligand binding to GPCR monomers and dimers with single molecule resolution by TIRF microscopy[33]. In the present study, we found that D_2 expressing CHO cells labeled with the antagonists **1a**,**b** showed a homogenous spot density and distribution, while our experiments with the agonists **2a**,**b** revealed the formation of clustered fluorescent puncta under TIRF illumination. Using a new approach based on the treatment with the mild reducing agent $NaBH_4$, we were able to convert fluorescent ligands bound to receptors at the cell surface to a non-fluorescent dark state[40,41]. In contrast, the clustered fluorescent puncta were inaccessible for the polar $NaBH_4$ and remained fluorescent. Since the fluorescent agonists **2a**,**b** stimulate substantial β-arrestin-2 recruitment and a comparable degree of receptor internalization in HEK cells transiently transfected with D_{2S} or D_{2L} receptors, we attributed these fluorescent clusters to internalized receptor ligand complexes.

Up to date, several methods have been employed to study receptor internalization. Very frequently, radioligand binding studies, ELISA- or immunofluorescence-based techniques and microplate-based functional whole cell assays have been used to quantify the proportion of internalized receptors[22–29]. Each of these methods has its own advantages and limitations. Classical radioligand binding studies require the availability of radioligands with distinct polarity and thus membrane permeability[24,46] to determine the fraction of extra- and intracellular receptors. In contrast, the surface-bound fraction of a radioligand or an antibody is removed under acidic conditions in the "acid wash" method. The remaining cell-bound fraction is considered to be internalized in acid-resistant compartments such as endosomes. Although this method has been widely used to investigate ligand-dependent GPCR internalization[47–50], it is not particularly suitable for dynamic analyses and fluorescence quantification, since not all compounds are washed off easily, requiring harsh treatment of the cells and cell membrane permeabilization[47,51]. Other methods such as ELISA or immunofluorescence require highly specific antibodies or adequately tagged receptors, complicating or even excluding their application to native cells or tissue. In addition, cells usually have to be fixed and/or permeabilized. Although intact living cells are used in microplate-based whole cell functional assays on first hand, the detection step often requires cell lysis. Moreover, these bulk measurements preclude single-cell or subcellular resolution.

The TIRF imaging approach in combination with our high affinity fluorescent dopamine receptor agonists and antagonists is compatible with the physiological conditions of ligand-receptor interaction, allowing the investigation of D_2 receptor internalization in living cells. Receptors are visualized in one single labeling step allowing for the monitoring of ligand binding and receptor trafficking. Treatment with $NaBH_4$ represents a mild, fast and efficient method to distinguish receptors on the cell surface from those in intracellular compartments without causing obvious changes in cell morphology. The relative extent of receptor internalization can be determined by comparison of the overall fluorescence intensity of the same living cell before and after treatment with the reducing agent. Although we have used CHO cells stably expressing our receptors of interest (D_{2S} and D_{2L}), TIRF microscopy using fluorescent ligands is generally applicable to cells endogenously expressing GPCRs[52]. Limitations of the approach include the relatively low throughput and the requirement of suitable fluorescently labeled agonists. Further, it should be acknowledged that due to the low penetration depth of the evanescent field (~100 nm) only a relative and no absolute quantification of receptors can be obtained.

Taking advantage of our new methodology, we have observed that the dopamine D_2 receptor isoforms, D_{2S} and D_{2L}, stably expressed in CHO cells, show differences in their internalization behavior. While approximately 32–35% of the detected D_{2S} receptors were found to be localized in intracellular compartments, only 16–20% of the observed D_{2L} receptors were found to internalize upon incubation with the fluorescent agonists **2a**,**b** for 1 h at 37 °C. Consistent with the present results, a number of previous studies have described that D_{2S} and D_{2L} receptors behave differently in their sensitivity to internalization/desensitization processes[24,34,46]. For instance, Itokawa *et al*. demonstrated in radioligand binding studies with stably transfected CHO cells that about 44% of surface expressed D_{2S} receptors became unavailable for the hydrophilic radioligand [^{3}H]sulpiride after incubation with the endogenous agonist dopamine. The internalization of D_{2L} was not only lower (22%), but also proceeded significantly slower (half-life of decrease 19 min for D_{2S} versus 33 min for D_{2L})[46]. Although to a lower overall extent, Kim *et al*. found a similar 2: 1 ratio for D_{2S} (20%) versus D_{2L} (10%) receptor internalization. In this case, internalization was determined as the decrease in [^{3}H]spiperone binding on the cell surface of transiently transfected CHO cells and found to be dependent on the expression of β-arrestin[24]. Using confocal microscopy, the same group observed a higher overall formation of endocytotic vesicles in D_{2S}-expressing cells compared to the D_{2L}-expressing counterparts upon agonist stimulation[24].

Interestingly, our ELISA-based internalization studies in transiently transfected HEK cells did not reveal significant differences between D_{2S} and D_{2L} receptor internalization. Similar observations have been previously described by Thibault *et al*. who employed a nearly identical protocol. However, this group still found enhanced D_{2S} internalization compared to D_{2L} upon heterologous desensitization in the same cell line[34]. Together these results suggest crucial influences of the employed cell types, transfection conditions and probably receptor expression levels on the highly regulated internalization process.

Importantly, D_{2S} and D_{2L} receptors share an extremely high sequence homology differing in only 29 additional amino acids within the third intracellular loop (ICL3) of D_{2L}[53]. Since the relatively long ICL3 has been previously reported to be important for D_2 receptor desensitization and trafficking[4,34,54], it is reasonable to assume that this region within ICL3 may attenuate receptor internalization and trafficking[5,24].

Previously, fluorescence microscopy based on immunohistochemistry staining has been used to measure the dynamics of agonist-induced D_2 receptor internalization *in vitro* in intact cells[55]. Furthermore, receptor adaptations have been studied by means of simultaneous positron emission tomography (PET) and functional magnetic resonance imaging (fMRI), giving access to non-invasive methods of studying receptor internalization *in vivo*[56]. The TIRF microscopy approach will allow to image native tissue with subcellular spatial resolution. Recent developments in the field of fluorescence microscopy will further promote the understanding of trafficking and regulation processes. As an example, multicolor imaging systems will facilitate a real time tracking of the dynamics of receptor-ligand complexes and their co-localization with various proteins involved in downstream signaling and internalization processes (e.g. agonist-receptor-G protein or agonist-receptor β-arrestin complexes) in living cells.

Methods

Cell culture. Chinese hamster ovary cells (CHO-K1) stably expressing human dopamine D_{2L}[57]or D_{2S}[57] receptors were maintained in DMEM/F12 medium supplemented with 10% fetal bovine serum (FBS), 2 mM L-glutamine, 1% penicillin-streptomycin, and 800 μg mL^{-1} geneticin (all cell culture reagents purchased from Invitrogen/Thermo Fisher Scientific) at 37 °C, 5% CO_2.

Glass slide cleaning. The glass slide cleaning procedure was carried out as described previously[33]. In brief, 18 mm No. 1 glass slides (Assistent) were extensively cleaned to remove any background fluorescence. First, they were sonicated in a solution containing 12% Decon 90 for 1 h. After three washes with Milli-Q filtered water, they were further sonicated in a solution of 5 M NaOH for 1 h and washed again three times with Milli-Q filtered water. Glass slides were then dried followed by sonication in chloroform for 1 h. Cleaned glass slides were dried and stored in 100% ethanol until usage.

Labeling and preparation for single-molecule TIRF microscopy imaging. 24 h before the TIRF experiment, glass slides were placed in a 12-well plate and coated with 20 µg ml^{-1} fibronectin (Sigma-Aldrich) in sterile dPBS (without Ca^{2+}/Mg^{2+}), for 1 h at 37 °C. After coating, fibronectin was aspirated and the glass surface was rinsed once with sterile dPBS (without Ca^{2+}/Mg^{2+}). CHO cells stably expressing dopamine D_{2L} or D_{2S} receptors were seeded on coated glass slides in phenol red-free DMEM/F12 supplemented with 10% FBS and were allowed to adhere overnight at 37 °C, 5% CO_2.

Fluorescent-ligand labeling. Cells were washed twice with phenol red-free DMEM/F12 supplemented with 10% FBS, labeled with a tenfold K_i value concentration of the corresponding fluorescent ligand and incubated unless otherwise stated at 37 °C and 5% CO_2 for 1 h. Specific labeling of the fluorescent ligands was confirmed by preincubation with 10 µM spiperone (a potent non-fluorescent dopamine D_2 receptor antagonist) for 2 h, followed by incubation with the fluorescent ligand as described above. Subsequently after labeling, cells were washed three times with phenol red-free DMEM/F12 supplemented with 10% FBS. Glass slides with labeled cells were placed in a custom-built imaging chamber (volume = 500 µL), washed twice with imaging buffer (137 mM NaCl, 5.4 mM KCl, 2.0 mM $CaCl_2$, 1.0 mM $MgCl_2$, and 10 mM HEPES, pH 7.4). Finally, the imaging chamber was refilled with fresh imaging buffer and mounted immediately on a microscope stage for TIRF microscopy imaging.

TIRF microscopy. TIRF microscopy was carried out as described previously[33]. In brief, experiments were performed at room temperature (24.0 ± 0.3 °C) on a motorized Nikon TI-Eclipse inverted microscope equipped with a 100x, 1.49 NA oil-immersion objective. Fluorescent dyes were excited using a Nikon D-Eclipse C1 laser box with 561 nm laser for TIRF microscopy. The laser light was filtered by an excitation filter 561/14 nm and directed by a dichroic long-pass mirror (cut-off wavelength 561 nm). The emitted light was passed through an emission bandpass filter 609/54 nm (Semrock Rochester), and was projected onto a water-cooled (Polar Series Accel 250 LC, Thermo Scientific) EM-CCD camera at −98 °C (512 × 512 FT, DU-897, Andor, UK). The microscope control and image acquisition was performed by the NIS Elements software (Nikon Instruments). To ensure homogenous illumination, only the central quarter of the chip (300 × 300 pixel) was used for imaging analysis. The gain of the EM-CCD camera was kept constant at 300, binning at 1 × 1, BitDepth at 14 bits, readout speed 10 MHz. Image sequences (5–500 frames) were acquired with an exposure time of 50 ms, resulting in the frame rate of 19.32 fps (frames per second).

Automated single particle tracking (ASPT). An automated single particle tracking (ASPT) algorithm[58] implemented in custom-written software, GMimPro (www.mashanov.uk), was used to identify and track individual fluorescent spots on sequential video frames to further determine their diffusive behavior. The procedure has been described previously in detail[33,43,59].

Calculation of the background corrected mean fluorescence intensity of single cells. Calculation of the mean background corrected fluorescence intensity $I(t)$ (arbitrary units) at time t of single cells for internalization experiments were performed as described previously[33]. In brief, regions of interest (ROI) were drawn around the membrane of an individual fluorescent cell (ROI_{cell}) and the background ($ROI_{background}$) outside the cell using Fiji software[57]. The total mean intensity over the entire cell area ($I(t)_{total\ cell}$) and the mean intensity over the background area ($I(t)_{bg}$) were measured and $I(t)$ were calculated as $I(t) = I(t)_{total\ cell} - I(t)_{bg}$.

Reductive treatment with sodium borohydride ($NaBH_4$). Samples of CHO cells stably expressing D_{2L} and D_{2S} receptors were prepared and labeled with the corresponding fluorescent ligands as described above. Labeled cells were treated with freshly prepared 30 mM $NaBH_4$ solution for 5 min and washed once with dPBS (with Ca^{2+}/Mg^{2+}). Finally the imaging chamber was refilled with fresh imaging buffer and image acquisition was performed under TIRF illumination at 561 nm. The entire process was conducted on the microscope stage so that the same cells could be imaged before and after the reductive treatment.

Internalization studies based on TIRF microscopy imaging. The mean fluorescence intensity (background corrected) of a fluorescent ligand labeled cell after $NaBH_4$ treatment was used to estimate internalized fluorescence as a percentage of the mean fluorescence intensity (background corrected) of a labeled cell before $NaBH_4$ reduction. Mean values and s.e.m were calculated from 9–24 cells from at least three independent experiments using Prism 6.0 (GraphPad Software, Inc.). Unpaired two-tailed Student's t-tests were used to determine statistical significance.

Measurement of emission spectra. To characterize the emission behaviour of the fluorescent ligand **1a** in the absence and presence of $NaBH_4$ (30 mM, 5 min) emission spectra were recorded on a CLARIOstar multimode microplate reader (BMG Labtech, λ_{ex} of 530 nm) using black, clear bottom 96-well plates (Greiner Bio-One) and the ligand diluted in dPBS (with Ca^{2+}/Mg^{2+}, pH 7.4) to a concentration of 1 µM.

Quantification of internalization by cell surface ELISA. Ligand-stimulated receptor internalization was quantified in analogy to a previously described procedure[34]. Briefly, HEK293T cells were transiently

transfected in suspension with plasmids (pcDNA 3.1) encoding $D_{2S}R$ or $D_{2L}R$ fused to a FLAG-epitope at their N-terminus together with a plasmid encoding GRK2 (3:1 receptor to GRK2 ratio), using polyethyleneimine as transfection reagent[60]. Transfected cells were transferred into 48-well plates (65,000 cells/well) pretreated with Poly-D-Lysine and maintained at 37 °C, 5% CO_2 for 48 h. After stimulation with the ligands dissolved in complete growth medium for 1 h at 37 °C, incubations were terminated by removal of the medium and fixation with 4% PFA (10 min, room temperature). Subsequently, cells were washed with washing buffer (150 mM NaCl, 25 mM Tris, pH 7.5), blocked for 1 h (3% skim milk powder in washing buffer) and incubated with the primary antibody (mouse anti-FLAG M2, 1:4,000, Sigma-Aldrich) for 1 h at room temperature. Cells were washed twice and blocked again before incubation with the horseradish peroxidase-conjugated secondary antibody for 1 h (HRP-rabbit anti mouse IgG, 1:20,000, Sigma-Aldrich). After three washing steps, 200 µL of a peroxidase substrate-containing solution (2.8 mM *o*-phenylenediamine in 35 mM citric acid, 66 mM Na_2HPO_4, pH 5.0) were added. Reactions were terminated after 30 min by addition of 200 µL 1 M H_2SO_4. From each well, 200 µL were transferred into a 96-well plate for absorbance readings at 492 nm on a CLARIOstar microplate reader. Data were analyzed by subtraction of the background (nontransfected cells) and normalization to control conditions (growth medium with 0.1% DMSO).

β-Arrestin-2 recruitment assay. The measurement of β -arrestin-2 recruitment to activated-receptors was performed utilizing the PathHunter assay (DiscoverX, Birmingham, UK) as described previously[60]. HEK293 cells stably expressing the EA-tagged β-arrestin-2 fusion protein (provided by DiscoverX) were transiently transfected with the ProLink(ARMS2-PK2)-tagged dopamine D_{2S} or D_{2L} receptors, respectively, using Mirus TransIT-293 (Mobitech, Göttingen, Germany) transfection reagent. 24 h after transfection, cells were detached using Versene (Invitrogen) and 5,000 cells per well were seeded into white, clear bottom 384-well plates (Greiner Bio-One) and maintained at 37 °C, 5% CO_2 for 24 h in assay medium. After incubation with different concentrations of test compounds (from 10^{-12} to 10^{-5} M final concentration) in duplicates for 5 h, the detection mix was added and incubation was continued for further 60 min. Chemiluminescence was determined on a CLARIOstar microplate reader. Resulting responses were normalized to the maximum effect obtained with quinpirole (100%) and the basal response (vehicle, 0%). Dose–response curves were calculated by nonlinear regression using the algorithms of Prism 6.0.

Data availability. The data that support the findings of this study are available within the Supplementary Information files and/or from the corresponding authors upon request.

References

1. Lagerstrom, M. C. & Schioth, H. B. Structural diversity of G protein-coupled receptors and significance for drug discovery. *Nat. Rev. Drug Discovery* **7**, 339–357 (2008).
2. Wise, A., Gearing, K. & Rees, S. Target validation of G-protein coupled receptors. *Drug Discovery Today* **7**, 235–246 (2002).
3. Namkung, Y. & Sibley, D. R. Protein kinase C mediates phosphorylation, desensitization, and trafficking of the D2 dopamine receptor. *J. Biol. Chem.* **279**, 49533–49541 (2004).
4. Clayton, C. C., Donthamsetti, P., Lambert, N. A., Javitch, J. A. & Neve, K. A. Mutation of three residues in the third intracellular loop of the dopamine D2 receptor creates an internalization-defective receptor. *J. Biol. Chem.* **289**, 33663–33675 (2014).
5. Neve, K. A. *The dopamine receptors*. 2nd edn, (Humana Press, 2010).
6. Davis, K. L., Kahn, R. S., Ko, G. & Davidson, M. Dopamine in schizophrenia: a review and reconceptualization. *Am. J. Psychiatry.* **148**, 1474–1486 (1991).
7. Zhang, A., Neumeyer, J. L. & Baldessarini, R. J. Recent progress in development of dopamine receptor subtype-selective agents: potential therapeutics for neurological and psychiatric disorders. *Chem. Rev.* **107**, 274–302 (2007).
8. Beaulieu, J.-M. & Gainetdinov, R. R. The physiology, signaling, and pharmacology of dopamine receptors. *Pharmacol. Rev.* **63**, 182–217 (2011).
9. De Mei, C., Ramos, M., Iitaka, C. & Borrelli, E. Getting specialized: presynaptic and postsynaptic dopamine D2 receptors. *Curr. Opin. Pharmacol.* **9**, 53–58 (2009).
10. Moore, C. A., Milano, S. K. & Benovic, J. L. Regulation of receptor trafficking by GRKs and arrestins. *Annu. Rev. Physiol.* **69**, 451–482 (2007).
11. Hanyaloglu, A. C. & von Zastrow, M. Regulation of GPCRs by endocytic membrane trafficking and its potential implications. *Annu. Rev. Pharmacol. Toxicol.* **48**, 537–568 (2008).
12. Tesmer, J. J. G. Hitchhiking on the heptahelical highway: structure and function of 7TM receptor complexes. *Nat. Rev. Mol. Cell Biol.* **17**, 439–450 (2016).
13. Luttrell, L. M. & Lefkowitz, R. J. The role of β-arrestins in the termination and transduction of G-protein-coupled receptor signals. *J. Cell Sci.* **115**, 455–465 (2002).
14. Goodman, O. B. *et al*. β-Arrestin acts as a clathrin adaptor in endocytosis of the β2-adrenergic receptor. *Nature* **383**, 447–450 (1996).
15. Laporte, S. A. *et al*. The β2-adrenergic receptor/βarrestin complex recruits the clathrin adaptor AP-2 during endocytosis. *Proc. Natl. Acad. Sci. USA* **96**, 3712–3717 (1999).
16. Ferguson, S. S. G. Evolving concepts in G protein-coupled receptor endocytosis: the role in receptor desensitization and signaling. *Pharmacol. Rev.* **53**, 1–24 (2001).
17. Tsao, P. & von Zastrow, M. Downregulation of G protein-coupled receptors. *Curr. Opin. Neurobiol.* **10**, 365–369 (2000).
18. Irannejad, R. *et al*. Conformational biosensors reveal GPCR signalling from endosomes. *Nature* **495**, 534–538 (2013).
19. Vilardaga, J.-P., Jean-Alphonse, F. G. & Gardella, T. J. Endosomal generation of cAMP in GPCR signaling. *Nat. Chem. Biol.* **10**, 700–706 (2014).
20. Calebiro, D., Nikolaev, V. O., Persani, L. & Lohse, M. J. Signaling by internalized G-protein-coupled receptors. *Trends Pharmacol. Sci.* **31**, 221–228 (2010).
21. Murphy, J. E., Padilla, B. E., Hasdemir, B., Cottrell, G. S. & Bunnett, N. W. Endosomes: A legitimate platform for the signaling train. *Proc. Natl. Acad. Sci. USA* **106**, 17615–17622 (2009).
22. Dado, R. J., Law, P. Y., Loh, H. H. & Elde, R. Immunofluorescent identification of a delta (delta)-opioid receptor on primary afferent nerve terminals. *Neuroreport* **5**, 341–344 (1993).
23. Skinbjerg, M. *et al*. Arrestin3 mediates D2 dopamine receptor internalization. *Synapse* **63**, 621–624 (2009).
24. Kim, S. J., Kim, M. Y., Lee, E. J., Ahn, Y. S. & Baik, J. H. Distinct regulation of internalization and mitogen-activated protein kinase activation by two isoforms of the dopamine D2 receptor. *Mol. Endocrinol.* **18**, 640–652 (2004).
25. Lam, V. M., Beerepoot, P., Angers, S. & Salahpour, A. A novel assay for measurement of membrane-protein surface expression using a beta-lactamase. *Traffic* **14**, 778–784 (2013).

26. Alvarez-Curto, E. *et al*. Developing chemical genetic approaches to explore G protein-coupled receptor function: validation of the use of a receptor activated solely by synthetic ligand (RASSL). *Mol. Pharmacol.* **80**, 1033–1046 (2011).
27. Hamdan, F. F., Audet, M., Garneau, P., Pelletier, J. & Bouvier, M. High-throughput screening of G protein-coupled receptor antagonists using a bioluminescence resonance energy transfer 1-based beta-arrestin2 recruitment assay. *J. Biomol. Screening* **10**, 463–475 (2005).
28. Milligan, G. Exploring the dynamics of regulation of G protein-coupled receptors using green fluorescent protein. *Br. J. Pharmacol.* **128**, 501–510 (1999).
29. Ashby, M. C., Ibaraki, K. & Henley, J. M. It's green outside: tracking cell surface proteins with pH-sensitive GFP. *Trends Neurosci.* **27**, 257–261 (2004).
30. Stoddart, L. A., Kilpatrick, L. E., Briddon, S. J. & Hill, S. J. Probing the pharmacology of G protein-coupled receptors with fluorescent ligands. *Neuropharmacology* **98**, 48–57 (2015).
31. Steyer, J. A. & Almers, W. A real-time view of life within 100 nm of the plasma membrane. *Nat. Rev. Mol. Cell Biol.* **2**, 268–275 (2001).
32. Poulter, N. S., Pitkeathly, W. T., Smith, P. J. & Rappoport, J. Z. The physical basis of total internal reflection fluorescence (TIRF) microscopy and its cellular applications. *Methods Mol. Biol.* **1251**, 1–23 (2015).
33. Tabor, A. *et al*. Visualization and ligand-induced modulation of dopamine receptor dimerization at the single molecule level. *Sci. Rep.* **6**, 33233 (2016).
34. Thibault, D., Albert, P. R., Pineyro, G. & Trudeau, L. E. Neurotensin triggers dopamine D2 receptor desensitization through a protein kinase C and beta-arrestin1-dependent mechanism. *J. Biol. Chem.* **286**, 9174–9184 (2011).
35. Oakley, R. H., Laporte, S. A., Holt, J. A., Caron, M. G. & Barak, L. S. Differential affinities of visual arrestin, βarrestin1, and βarrestin2 for G protein-coupled receptors delineate two major classes of receptors. *J. Biol. Chem.* **275**, 17201–17210 (2000).
36. Salahpour, A. *et al*. BRET biosensors to study GPCR biology, pharmacology, and signal transduction. *Front. Endocrinol.* **3**, 105 (2012).
37. Macey, T. A., Liu, Y., Gurevich, V. V. & Neve, K. A. Dopamine D1 receptor interaction with arrestin3 in neostriatal neurons. *J. Neurochem.* **93**, 128–134 (2005).
38. Merriam, L. A. *et al*. Pituitary adenylate cyclase 1 receptor internalization and endosomal signaling mediate the pituitary adenylate cyclase activating polypeptide-induced increase in guinea pig cardiac neuron excitability. *J. Neurosci.* **33**, 4614–4622 (2013).
39. Teng, H. B. & Wilkinson, R. S. 'Delayed' endocytosis is regulated by extracellular Ca2+ in snake motor boutons. *J. Physiol. London* **551**, 103–114 (2003).
40. Kundu, K. *et al*. Hydrocyanines: a class of fluorescent sensors that can image reactive oxygen species in cell culture, tissue, and *in vivo*. *Angew. Chem. Int. Ed. Engl.* **48**, 299–303 (2009).
41. Vaughan, J. C., Jia, S. & Zhuang, X. Ultrabright photoactivatable fluorophores created by reductive caging. *Nat. Methods* **9**, 1181–1184 (2012).
42. Kasai, R. S. & Kusumi, A. Single-molecule imaging revealed dynamic GPCR dimerization. *Curr. Opin. Cell. Biol.* **27**, 78–86 (2014).
43. Hern, J. A. *et al*. Formation and dissociation of M1 muscarinic receptor dimers seen by total internal reflection fluorescence imaging of single molecules. *Proc. Natl. Acad. Sci. USA* **107**, 2693–2698 (2010).
44. Calebiro, D. *et al*. Single-molecule analysis of fluorescently labeled G-protein–coupled receptors reveals complexes with distinct dynamics and organization. *Proc. Natl. Acad. Sci. USA* **110**, 743–748 (2013).
45. Yudowski, G. A. & von Zastrow, M. Investigating G protein-coupled receptor endocytosis and trafficking by TIR-FM. *Methods Mol. Biol.* **756**, 325–332 (2011).
46. Itokawa, M. *et al*. Sequestration of the short and long isoforms of dopamine D2 receptors expressed in Chinese hamster ovary cells. *Mol. Pharmacol.* **49**, 560–566 (1996).
47. Nouel, D. *et al*. Differential internalization of somatostatin in COS-7 cells transfected with SST1 and SST2 receptor subtypes: a confocal microscopic study using novel fluorescent somatostatin derivatives. *Endocrinology* **138**, 296–306 (1997).
48. Pheng, L. H. *et al*. Agonist- and antagonist-induced sequestration/internalization of neuropeptide Y Y1 receptors in HEK293 cells. *Br. J. Pharmacol.* **139**, 695–704 (2003).
49. Dutta, D., Williamson, C. D., Cole, N. B. & Donaldson, J. G. Pitstop 2 is a potent inhibitor of clathrin-independent endocytosis. *PLoS One* **7**, e45799 (2012).
50. Benn, A., Bredow, C., Casanova, I., Vukicevic, S. & Knaus, P. VE-cadherin facilitates BMP-induced endothelial cell permeability and signaling. *J. Cell Sci.* **129**, 206–218 (2016).
51. Lee, M. C., Cahill, C. M., Vincent, J. P. & Beaudet, A. Internalization and trafficking of opioid receptor ligands in rat cortical neurons. *Synapse* **43**, 102–111 (2002).
52. Nenasheva, T. A. *et al*. Abundance, distribution, mobility and oligomeric state of M2 muscarinic acetylcholine receptors in live cardiac muscle. *J. Mol. Cell. Cardiol.* **57**, 129–136 (2013).
53. Dal Toso, R. *et al*. The dopamine D2 receptor: two molecular forms generated by alternative splicing. *The EMBO Journal* **8**, 4025–4034 (1989).
54. Kim, K.-M. *et al*. Differential Regulation of the Dopamine D2 and D3 Receptors by G Protein-coupled Receptor Kinases and β-Arrestins. *J. Biol. Chem.* **276**, 37409–37414 (2001).
55. Guo, N. *et al*. Impact of D2 receptor internalization on binding affinity of neuroimaging radiotracers. *Neuropsychopharmacology* **35**, 806–817 (2010).
56. Sander, C. Y., Hooker, J. M., Catana, C., Rosen, B. R. & Mandeville, J. B. Imaging agonist-induced D2/D3 receptor desensitization and internalization *in vivo* with PET/fMRI. *Neuropsychopharmacology* **41**, 1427–1436 (2016).
57. Hayes, G., Biden, T. J., Selbie, L. A. & Shine, J. Structural subtypes of the dopamine D2 receptor are functionally distinct: expression of the cloned D2A and D2B subtypes in a heterologous cell line. *Mol. Endocrinol.* **6**, 920–926 (1992).
58. Mashanov, G. I. & Molloy, J. E. Automatic detection of single fluorophores in live cells. *Biophys. J.* **92**, 2199–2211 (2007).
59. Mashanov, G. I., Tacon, D., Knight, A. E., Peckham, M. & Molloy, J. E. Visualizing single molecules inside living cells using total internal reflection fluorescence microscopy. *Methods* **29**, 142–152 (2003).
60. Möller, D. *et al*. Discovery of G protein-biased dopaminergics with a pyrazolo[1,5-a]pyridine substructure. *J. Med. Chem.* **60**, 2908–2929 (2017).

Acknowledgements

This work was supported by the German Research Foundation (DFG 13/8-2, GRK1910). We thank Prof. Dr. Michel Bouvier (IRIC, Montréal, Canada) for providing the cDNA encoding the human isoform of GRK2.

Author Contributions

A.T. designed, conducted and analyzed the TIRF experiments and wrote the manuscript. D.M. performed and analysed ELISA internalization experiments and wrote the manuscript. H.H. performed and analyzed β-arrestin recruitment experiments. J.K. contributed to the methodology. P.G. was responsible for the overall project strategy, provided project supervision and wrote the manuscript.

Additional Information

Supplementary information accompanies this paper at doi:10.1038/s41598-017-11436-1

Competing Interests: The authors declare that they have no competing interests.

Publisher's note: Springer Nature remains neutral with regard to jurisdictional claims in published maps and institutional affiliations.